Daagu International Journal of Basic and Applied Research 5(2023): 120-143
DOI: https://doi.org/10.20372/DIJBAR.530500

Original Research

Ascertaining the source of major dissolved solute and recharge mechanism of groundwater in the Golina River Basin, Northern Ethiopia

Hindeya Gebru[1,2*], Tesfamichael Gebreyohannes[2], and Ermias Hagos[2]

[1] Department of Earth Sciences, Samara University, Samara, Ethiopia

[2] School of Earth Sciences, Mekelle University, Mekelle, Ethiopia

*Corresponding author: hindualem@gmail.com

Abstract

This study uses major ions and stable water isotopes to understand the solute acquisition, origin, and recharge mechanisms of groundwater of the alluvial deposits (sand and gravels) and weathered and fractured volcanic rocks aquifers in the Golina River Basin (GRB), Ethiopia. The results of the hydrogeochemistry indicates that the solutes of the groundwater are dominantly acquiring by the natural weathering of Ca^{2+} and Mg^{2+}-rich silicate minerals. The study suggest that groundwater preferentially flow through the basalts and little through the acidic rocks which determine the four groundwater facies (Ca^{2+}–HCO_3^-, Mg^{2+}–HCO_3^-, Ca^{2+}–Mg^{2+}–HCO_3^-, and Na^+–HCO_3^-) in the area. Further, there is an ion exchange between groundwater and its host environment during the movement process, creating disequilibrium within the aquifer. Based on the similarity of their hydrochemical properties, the groundwater in the area is grouped into four major groups and four subgroups. The stable water isotopes results suggest that seasonal variances in the slope and intercepts of the local meteoric water line (LMWL) is associated with changes in meteorology and moisture sources, which underlie the subtle variations in $\delta^{18}O$ and δ^2H in precipitation over time and space. The seasonal local meteoric water lines of the Golina River Basin were obtained; resulting $\delta^2H = 7.3\pm4.4\delta^{18}O +8.8\pm1$ for wet season precipitations (months between June and September) and $\delta^2H = 4.5\pm3.5\delta^{18}O +11.6\pm1.1$ for dry season precipitations (months between October to May). The study further reveals that groundwater exhibits lower slope (5.1±2) and lower intercept (5.6±0.77) than LMWL and that of GMWL, indicating the evaporation of infiltrating meteoric waters before it joining the aquifer system. Therefore, the present study finds that groundwater is recharged from direct infiltration of the precipitation and recharged from the nearby mountainous regions on west and east of the basin.

Keywords: Solute source, groundwater recharge, stable water isotopes, Golina River Basin

©*Daagu International Journal of Basic and Applied Research*

Citation: Gebru, H., Gebreyohannes, T. and Hagos, E. 2023. Ascertaining the source of major dissolved solute and recharge mechanism of groundwater in the Golina River Basin, Northern Ethiopia. *Daagu International Journal of Basic and Applied Research*, 5(1): 120-143. DOI: https://doi.org/10.20372/DIJBAR.530500.

1. INTRODUCTION

The primary chemical composition of groundwater is the compound of hydrogen and oxygen ions which is H_2O (Candela & Morell, 2009). However, the chemical composition of the groundwater is changed as a result of chemical reaction taking place in the atmosphere when it rain and it continues to react with unsaturated, and saturated water-bearing formations through the groundwater movement. The chemical composition of groundwater changes through the groundwater flow paths. The groundwater chemistry is mainly affected by natural conditions such as aquifer lithology, groundwater recharge sources, water-sediment interaction, by anthropologic activities such as urbanization, industry, and agriculture, as well as by atmospheric input (Tóth, 1999; Helena et al., 2000; Redwan & Abdel Moneim, 2016).

The stable isotopes of Oxygen and Hydrogen are effective tracers of water sources because they are constituents, and move with water molecules (Craig, 1961; Dansgaard, 1964; Gat, 1996; Kendall & Coplen, 2001; Kuang et al., 2019). Therefore, their behavior and variations reflect the origin of, and the hydrological and geochemical processes undergone by, natural water bodies (Clark & Fritz, 1997; Gonfiantini, 1998; Jeelani et al., 2018). In a particular environment, precipitation exhibits a characteristic isotopic signature that can be used as a tracer for understanding atmospheric circulation patterns (Hoffmann et al., 2000; Birks et al., 2002), and history of water fluxes to, from, and between air masses as they travel across continents (Liu et al., 2010). In addition to inspiring a wide range of interpretations of hydrological processes at the surface and within aquifers (IAEA, 1983, 1989; Kehew, 2001; Aggarwal et al., 2005; Clark & Fritz, 2013; Kebede, 2013), which includes, the estimation of recharge processes, residence times, mixing processes, and delineation of recharge sources, etc., (Clark & Fritz, 1997; Fynn et al., 2016; Jeelani et al., 2017, 2018; McGuire et al., 2002; Price & Swart, 2006; Shah et al., 2017, 2022, 2023).

Since the 1960s, over 1000 monthly precipitation collection stations in more than 125 countries are monitored for the isotopic composition of precipitation by the Global Network for Isotopes in Precipitation (GNIP) which is operated by the International Atomic Energy Agency and the World Meteorological Organizations (IAEA/WMO). In Ethiopia, there is only one long term GNIP station, located in Addis Ababa, and most isotope related researches in the country use this station as a Local Meteorite Water Line (LMWL). However, a single location in Addis

Ababa cannot capture the long term hydrological and hydroclimate processes in the Ethiopia (Bedaso et al., 2019).

The hydrogeological and hydrochemical conditions in volcanic aquifers of the Ethiopian main rift valley were identified using the hydrochemical and stable isotopes of groundwater (Ayenew et al., 2008; Demlie et al., 2008; Kebede et al., 2005, 2008). (Alemayehu et al., 2011) studied the groundwater evolution of the basalt aquifer in Northern Ethiopian highlands in Axum using hydrochemistry and isotope evidence. Their finding suggested that groundwater in the Axum is of recent meteoric origin recharged by direct infiltration of local rainfall and through lateral flow in the recharge zone. (Ayenew et al., 2013) studied the groundwater origin of the Raya valley in Northern Ethiopia plateau and marginal graben using stable isotopes and the result indicated that the groundwater originated from meteoric but has undergone slight evaporated fractionation before recharge. (Girmay et al., 2015) studied the application of environmental isotopes for the conceptual groundwater flow model of the Tekeze River Basin in Northern Ethiopia. Their study revealed that the existence of shallow/local, intermediate and deep/semi-regional groundwater flow systems. There some more reported studies that provide information on the hydrogeochemical and isotopic characteristics of groundwater in the region; however, detailed insights into the sources of major solutes and recharge mechanism of groundwater from volcanic aquifers in the Golina River Basin (GRB) remain poorly understood. Hence, major gaps exist between data and understanding, and bridging this gap is key to understanding the groundwater system in the region. Towards this, the presents study aims to characterize the groundwater resources from the alluvial deposits and volcanic aquifers in the Golina River Basin by utilizing the major ions and stable water isotopes. The specific objectives of this study are 1) to identify the mineralization processes that determine the dissolved solutes in the groundwater, and 2) to comprehend the groundwater recharge mechanism of the area.

2. MATERIALS AND METHODS

2.1. Study area

This study examines groundwater resource from the alluvial deposits and volcanic aquifers in the Golina River Basin (GRB), which is located in the Amhara Regional State, Northern Ethiopia (Figure 1). The region covers an area of about 917 km^2 and is characterized by gentle to steep topography with elevation gradient ranging from 1337 to 3970 meters above mean sea level (m amsl). The perennial River Golina and seasonal Hormat and Kelkelit rivers shape the major drainage, and its pattern relates to regional topography. The Hormat and Kelkelit Rivers

merge with the River Golina and flow out of the basin in the west. The study region experiences semi-arid climate, and receives total precipitation of 903mm (Gebru et al., 2020). The Golina River Basin's geology is a part of the Tertiary Flood Basalts of the Northwestern Ethiopian Plateau, which were created before 30Mya during the Cenozoic era (Hofmann et al., 1997; Gebru et al., 2020). These volcanic formations are regrouped by (Gregnanin & Piccirillo, 1974; Zanettin & Justin-Visentin, 1973) as Ashangi and Aiba basalts, Alaje Rhyolites, and Termaber basalts. Rhyolite rock with flow bands covers the north-east corner of the research area (Figure 1). Greenish, fine-grained, slightly weathered, ridge-forming, compacted, and associated with ignimbrite, tuffs, and Ash are the characteristics of this rock unit. The porphyritic rhyolite rock contains K-feldspar, quartz, and plagioclase phenocrysts. Due to the northeast-moving sinistral strike-slip fault, the rhyolite rock is in contact with the Ashangi formation (Gebru et al., 2020). In the middle of the valley floor, granite appears as a ridge and hill making intrusive rocks. The granite rock that exposed in Golina River Basin has pinkish and greyish in fresh color, yellowish weathered color, medium to coarse-grained. Quartz, k-feldspar, and pyroxenes are the main compositions of the granite rock in the area. The alluvial deposits that contain gravels, sand, silt, and clay sediments are exposed in the graben formed by western and eastern ridges (Gebru et al., 2020). The grain size of the sediments is coarse near the mountainous while it is fine-grained in the central part of the graben (Valley floor). The stratigraphy of the sediments indicates that there were a series of sedimentation cycles.

Groundwater is primarily found in alluvial deposits; as a result, most boreholes drilled for domestic or irrigation purposes are found in these deposits; and the alluvial deposits are the main potential for the groundwater occurrence in the area (Gebru et al., 2020). The findings of Kebede (2013) shown that basal sequence (Ashangi basalt) is low permeability compared to the upper sequences (Aiba-Termaber-Alaji formations) of the Ethiopian volcanic plateau; while the rhyolite and granite which form ridges are impervious.

2.2. Data collection and analysis

Water samples from boreholes (n= 31), dug wells (n= 5), and springs (n= 2) were collected in high density polyethylene (HDPE) bottles for major ions and stable water isotopes analysis. As well, monthly cumulative rain water samples (n=18) were collected at Kobo Meteorological Station Centre (P1) for stable water isotopes. In addition, isotope data for seven (n=7) monthly cumulative rain water samples (available only for 2002) were obtained from the International Atomic Energy Agency (IAEA) (https://www.iaea.org). During water sampling in the

boreholes and dug wells, water was continuously pumped out for about ten minutes in an effort to avoid stagnant water sampling. In contrast, the cumulative rainwater sample was collected in a well-designed collector in such a way that can result in negligible evaporation (Figure 2).

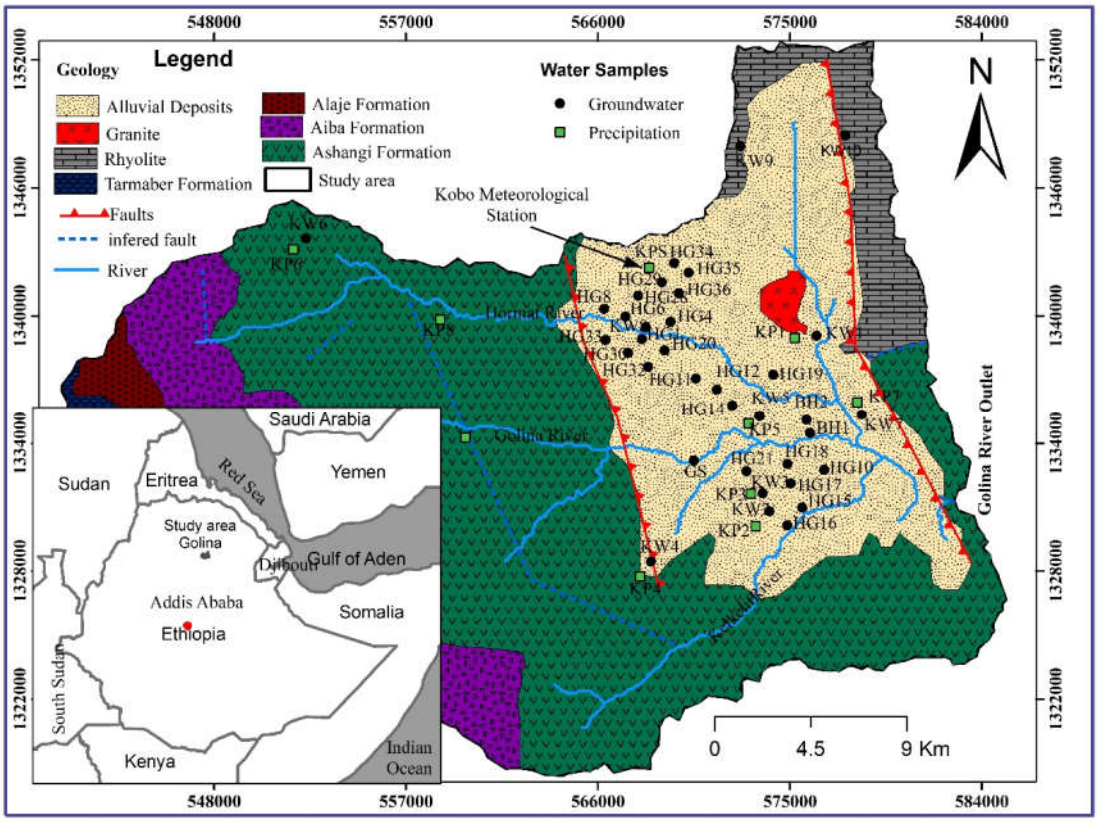


Figure 1. Map of the Golina River Basin, showing the geology and location of sampling sites

For major ions two separate aliquots were taken, the filtered samples (filtered through 0.45µm) determined for cation content were acidified with ultra-pure HNO_3 to lower pH < 2, whereas the unacidified samples were kept to determine anion concentration. The parameters like pH, EC and HCO_3^- were determined in the field using multi parameters test kits while Na^+, K^+, Ca^{2+}, Mg^{2+}, Cl^-, SO_4^{2-}, NO_3, NO_2^-, PO_4, and F^- were analyzed using Ion Chromatography (IC) in in the water laboratory at Technical University of Darmstadt (TUD). The measurement accuracy of ±5% were determined using the ion balance or electro-neutrality (EN) method (Matthess, 1982)-(Singhal & Gupta, 2010) using following equation (Eq. 1). The laboratory analysis result is acceptable if the electro-neutrality of any water sample is within ±5%.

$$EN = \frac{\sum \text{cation} - \sum anions}{\sum \text{Cations} + \sum anions} \times 100 \qquad \text{(Eq. 1)}$$

Pearson correlation matrix and hierarchical cluster analysis (HCA) were performed to distinguish the hydrogeochemical processes determining the dissolved solutes in the groundwater. Besides, Durov`s and various scatter diagrams were plotted, and Chloro-alkaline indices (CAI) and Gibbs ratios (Eq. 2-5) were also determined. Statistical Packages for the Social Sciences (SPSS) of (version-16) and Aquachem (version-4.0) software were used to evaluate all these statistical parameters.

$$\mathrm{CAI-I} = \frac{[\mathrm{Cl}-(\mathrm{Na}+\mathrm{K})]}{\mathrm{Cl}} \quad \text{(Eq. 2)}$$

$$\mathrm{CAI-II} = \frac{[\mathrm{Cl}-(\mathrm{Na}+\mathrm{K})]}{\mathrm{SO_4}+\mathrm{HCO_3}+\mathrm{CO_2}+\mathrm{NO_3}} \quad \text{(Eq. 3)}$$

$$Gibbs\ Ratio\ I = \frac{Cl^-}{Cl^-+HCO_3^-} \quad \text{(Eq. 4)}$$

$$Gibbs\ Ratio\ II = \frac{Na^+}{Na^++Ca^{2+}} \quad \text{(Eq. 5)}$$

Stable water isotope ($\delta^{18}O$ and $\delta^{2}H$) composition (expressed in per mill, ‰) in waters samples were measured relative to Vienna Standard Mean Ocean Water (V-SMOW) using δ notation (Eq. 6) by the L2130-*i*-PICARRO water isotopes and gas concentration analyzer in TUD water laboratory and by the Los Gatos Research (LGR) Liquid Water Isotopes Analyzer (LWIA) at School of Earth Sciences Isotope Laboratory, Addis Ababa University. For the accuracy of the laboratory result, raw data were corrected for sample-to-sample memory after three consecutive injections of each sample were measured; and the reported value represents the mean.

$$\delta_{Samples} = \frac{R_{Sample}-R_{Standard}}{R_{Standard}} \times 1000‰ \quad \text{(Eq. 6)}$$

Similarly, the linear relationship between hydrogen and oxygen isotopes distributions of precipitation (also known as GMWL) and secondary parameter known as d-excess (or d) were determined using the following equation (Eq. 7 and 8).

$$\delta^2H = 8\delta^{18}O + 10 \quad \text{(Eq. 7)}$$

$$d-excess = \delta^2H - 8\delta^{18}O \quad \text{(Eq. 8)}$$



Figure 2. Cumulative rainwater sample collection system

3. RESULT AND DISCUSSION

3.1. Hydrogeochemical characteristics and solute source

3.1.1. Correlation Coefficients

The correlation coefficient values range from +1 (strong positive correlation) to -1 (strong negative correlation) as indicated in Table 1. A high correlation is observed between the EC and TDS. EC has a strong positive correlation with HCO_3^-, alkalinity, Mg^{2+}, Cl^-, Ca^{2+}, NO_3^- and SO_4^{2-} and poor positive correlation with Na^+, K^+, and F^- but it has a negative correlation with pH values. TDS has a strong positive correlation mainly with HCO_3^-, SO_4^{2-}, Mg^{2+}, and Ca^{2+} which indicates the contributions of the anions and cations in overall mineralization and alkalinity. Most of the parameters have a negative correlation with pH values. F^- has a poor positive correlation with Cl^-, NO_3^-, SO_4^{2-}, Na^+, and K^+, and has a negative correlation with the other parameters. The positive correlation of Mg^{2+} with all EC, TDS, alkalinity, HCO_3^-, Cl^- and NO_3^- also observed and negative with pH and F^-. Na^+ has a strong positive correlation with Cl^- and SO_4^{2-}, poor positive correlation with EC, TDS, Alkalinity, HCO_3^-, F^-, NO_3^-, Mg^{2+}, Ca^{2+}, and K^+ and negative correlation with pH and PO_4^-. K+ has a poor positive correlation with all parameters except with Ca^{2+} which is a negative correlation. The strong positive correlation of NO_3^- with EC, Mg^{2+}, and Cl^-, poor positive correlation with Na^+, K^+, HCO_3^-, SO_4^{2-} and negative correlation with PO_4^- and pH which indicates NO_3^- sources are different which could be the agricultural activities such as fertilizers.

Table 1 Correlation matrix of the groundwater parameters (* is at significance level 0.05 and ** is at significance level of 0.01)

Parameters	EC	TDS	pH	HCO_3^-	F^-	Cl^-	NO_3^-	PO_4^-	SO_4^{2-}	Na^+	K^+	Mg^{2+}	Ca^{2+}	Alkalinity
EC	1.00													
TDS	0.79**	1.00												
pH	-0.27	-0.40*	1.00											
HCO_3^-	0.81**	0.76**	-0.23	1.00										
F^-	0.14	0.02	0.02	-0.08	1.00									
Cl^-	0.63**	0.40*	-0.10	0.61**	0.14	1.00								
NO_3^-	0.55**	0.34	-0.01	0.47**	0.01	0.68**	1.00							
PO_4^-	0.10	0.08	-0.20	0.08	-0.23	-0.16	-0.12	1.00						
SO_4^{2-}	0.55**	0.58**	-0.27	0.37*	0.10	0.67	0.44*	-0.05	1.00					
Na^+	0.45**	0.38*	-0.02	0.35**	0.26	0.73**	0.40*	-0.22	0.71**	1.00				
K^+	0.34	0.25	0.43*	0.28	0.43*	0.24	0.28	0.09	0.07	0.22	1.00			
Mg^{2+}	0.74**	0.57**	-0.03	0.73**	-0.05	0.57	0.66**	0.21	0.30	0.27	0.39*	1.00		
Ca^{2+}	0.60**	0.66**	-0.45**	0.74**	-0.11	0.47**	0.22	0.05	0.51**	0.17	-0.03	0.27	1.00	
Alkalinity	0.75**	0.93**	-0.35*	0.87**	-0.07	0.29	0.26	0.12	0.31	0.20	0.24	0.60**	0.67**	1.00

3.1.2. Molar Ratios

For this purpose, we can use the ratios between magnesium (Mg^{2+}) and calcium (Ca^{2+}) which varies from 0.17 to 3.07. All groundwater samples (Except sample KW8 and KW9) show a ratio of less than 2, which indicates that silicate mineral dissolution contributes calcium and magnesium to the groundwater in the study area. As the Ca^{2+} vs Mg^{2+} plot (Figure 3a) shows, some of the groundwater samples lie below the line 1:1 ratio while some of them fall above this line which shows the contribution of the silicate minerals to the groundwater chemistry is from both calcium and magnesium-rich pyroxene and olivine minerals in basalt (Singhal & Gupta, 2010). All groundwater samples (except samples of GS, BH1, and KW6) lie below the 1:1 line of $Na^+ + K^+$ vs $Ca^{2+} + Mg^{2+}$ plot, which indicates that the groundwater chemistry is influenced by the minerals of basic rock (Basalts). The samples falling above the 1:1 line could be originating from the acidic rocks associated with the tertiary volcanic rocks in the study area (Figure 3b). The Ca + Mg vs total cations and $Na^+ + K^+$ vs total cations graph show that silicate minerals of the volcanic rocks in the study area contribute mainly calcium and magnesium ions to the groundwater (Figure 3c and d). The basalts exposed in the study area are composed of mainly pyroxene, olivine, and plagioclases as a groundmass as well as phenocrysts. Therefore. the groundwater composition is evolved from the calcium and magnesium-rich silicate mineral weathering. The chemical composition of the groundwater which is sodium-rich may origin from the acidic rocks that are exposed in the area (granite and rhyolite) and from the associated acidic rocks with tertiary volcanic rocks (e.g., Alaje formation contains ignimbrite and trachyte).

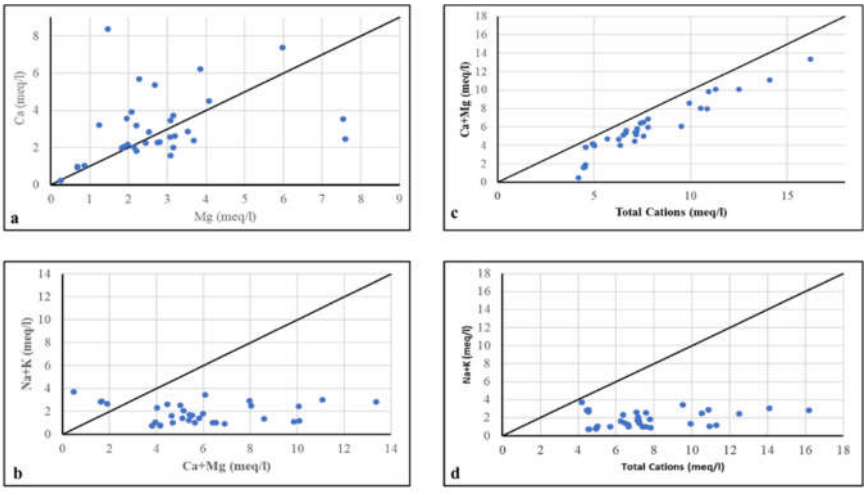


Figure 3 a) Ca vs Mg, b) $Na^+ + K^+$ vs $Ca^{2+} + Mg^{2+}$, c) $Ca^{2+} + Mg^{2+}$ vs total cations d) and $Na^+ + K^+$ vs total cations plots

The Ca^{2+} + Mg^{2+} vs HCO_3^- + SO_4^{2-} plot shows most of the groundwater samples tend to be around and below the 1:1 line due to excess in HCO_3^- and SO_4^{2-} as a result of ion exchanges between the groundwater ions and aquifer materials (Figure 4a and b). It indicates the groundwater sources are from silicate weathering rather than carbonate weathering (Bawoke et al., 2019). In Na^++K^+ vs Cl^- plot (Figure 4c), all groundwater samples lie on the left side and above the 1:1 line which indicates that there are no additional sources of chloride to the groundwater like salt intrusions and therefore the sodium released is from ion-exchange reactions with silicate minerals weathering (Kumar et al., 2009; Meybeck, 1987).

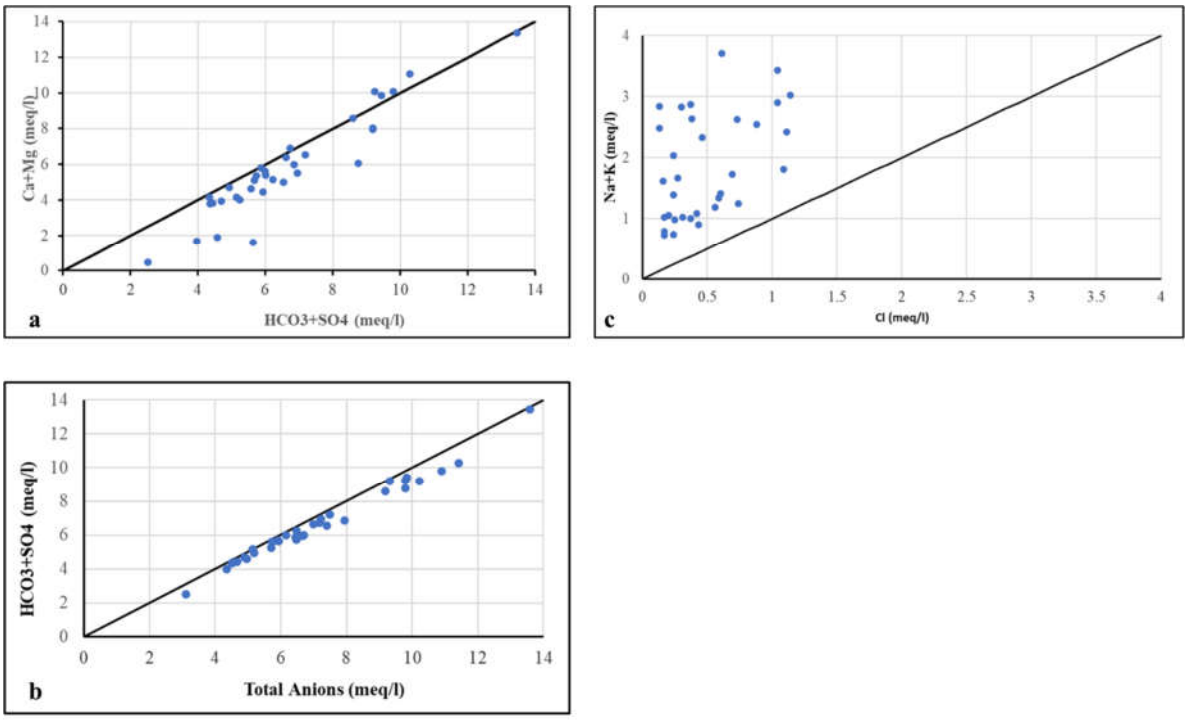


Figure 4. a) Ca^{2+}+Mg^{2+} vs HCO_3^-+SO_{42-}, b) HCO_3^-+SO_4^{2-} vs total anions and c) Na^++K^+ vs Cl^- pots

3.1.3. Hydrochemical Processes (Durov's Diagram)

Hydrochemical facies of the groundwater in the Golina River Basin is dominated by Ca^{2+}-Mg^{2+}-HCO_3 and Mg^{2+}-Ca^{2+}-HCO_3^- water types with minor Na^+-Ca^{2+}-HCO_3^- and Ca^{2+}-Na^+-HCO_3^- (Figure 5). Except for sample of GS from spring, all groundwater samples are displayed on the ion exchanges between the ions in groundwater and the aquifer materials. The GS spring sample is laid on the simple dissolution, clearly observed in the field which is mixed with the Golina river water (Figure 5).

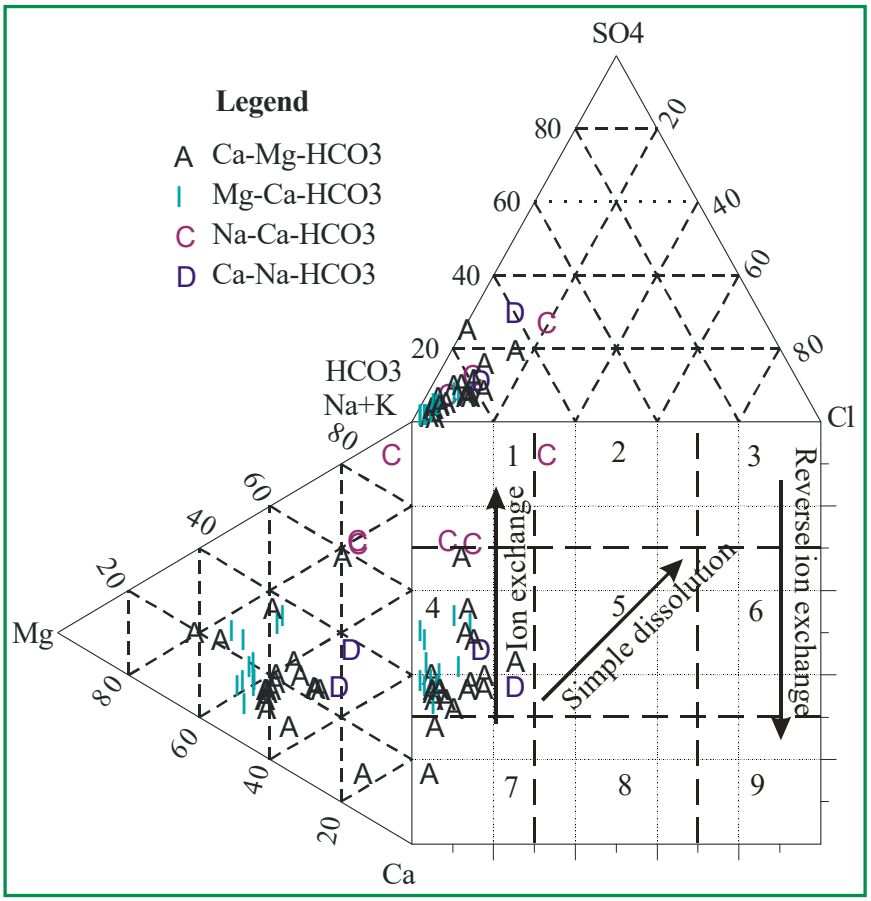


Figure 5. Durov's Diagram for water types and hydrochemical processes

3.1.4. Mechanisms controlling groundwater chemistry

According to Gibbs (1970) discussion, there are three mechanisms controlling world water chemistry namely atmospheric precipitation, rock dominance, and evaporation-fractional crystallization processes that affect the hydrogeochemical processes. These classifications have a vital role in the determination of groundwater sources and to establish the relationship between the water composition and the aquifer lithological characteristics (Kumar et al., 2015). The results of the Gibbs ratios were plotted with total dissolved solids (TDS) in mg/l as shown in Figure 6. Accordingly, the groundwater chemistry controlling mechanism of the samples from the study area was indicated to be the rock dominance. This result reflected that the water, rock and soil interaction are the main controlling factor for the hydrochemical evolution in the area.

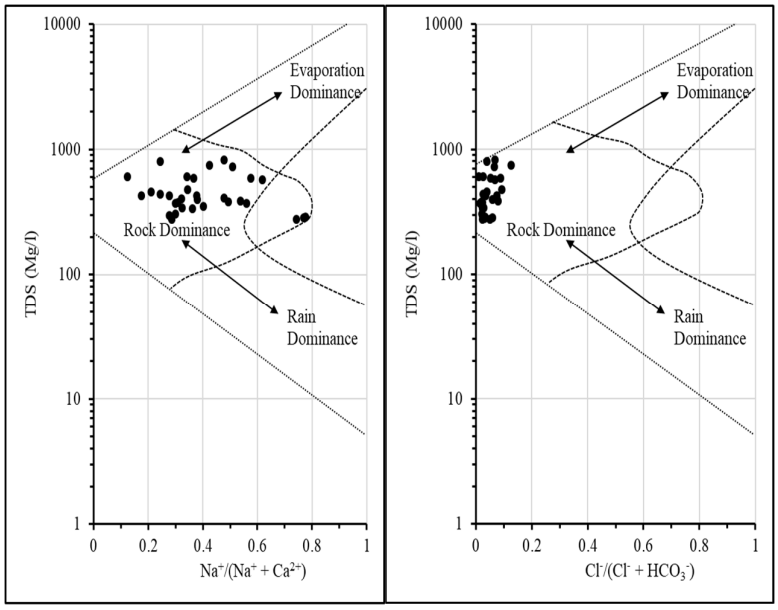


Figure 6. Gibbs diagrams of TDS Vs $Na^+/(Na^+ + Ca^{2+})$ (Left side) and TDS Vs $Cl^-/(Cl^- + HCO_3^-)$ (Right side)

3.1.5. Chloro-alkaline Indexes

Schoeller (1967) proposed chloro-alkaline indexes CAI- I and -II to indicate the ion exchange between groundwater and its host environment. Both indexes are deducted from the cation ions exchange between groundwater and aquifer materials. Both CAI-I and II can be positive when the ion exchange between Mg^{2+} and Ca^{2+} from the aquifer material with Na^+ and K^+ from the water whereas negative when the Na^+ and K^+ from the aquifer material with the cations of Ca^{2+} and Mg^{2+} from the groundwater. In all conditions of CAI-I and CAI-II (Figures 7 and 8), all of groundwater samples are falling under negative ratios of ion exchange which indicates there is cation-anion exchange and shows chloro-alkaline disequilibrium.

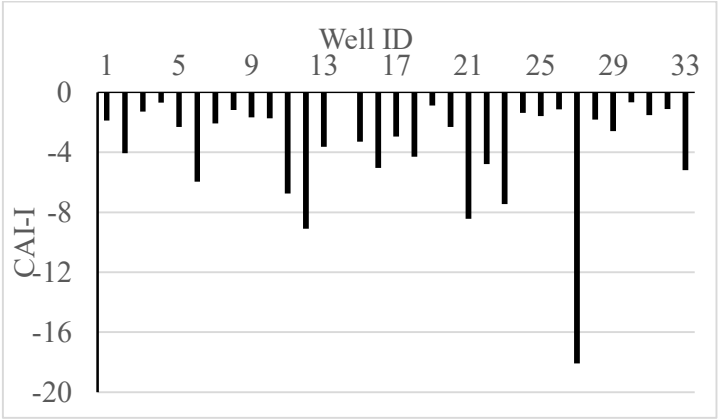


Figure 7. Chloro-alkaline-I of the groundwater samples

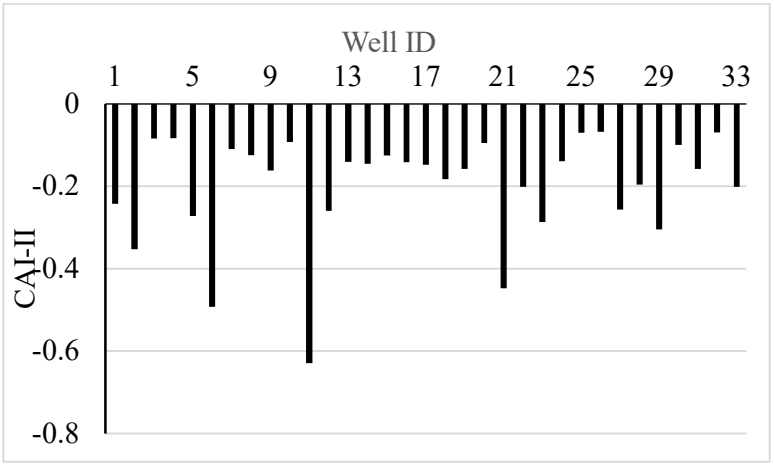


Figure 8. Chloro-alkaline-II of the groundwater samples

3.1.6. Hierarchal Cluster analysis (HCA)

Hierarchal cluster analysis was used to classify the groundwater samples based on the similarity of their parameters. The groundwater samples are grouped into four major categories and each of the major groups is clustered into subgroups based on the physicochemical parameters (Figure 9). The Dendrogram plot was developed based on the Wards cluster and square Euclidian distance methods (Belkhiri & Mouni, 2012). Data of EC and pH, major cations of Na^+, K^+, Ca^{2+}, Mg^{2+}, and major anions of Cl^-, SO_4^{2-}, NO_3^-, and HCO_3^- of the 34 groundwater samples were used to categorize using hierarchal cluster analysis. Accordingly, four major hierarchal taxonomies (G1, G2, G3, and G4) and subgroups (G2SB1, G2SB2, G4SB1, and G4SB2) have been identified based on a references line (Phenon line) with a rescaled distance of 6. The first Group (G1) is categorized based on the elevated values of EC, TDS, Na^+, Mg^{2+}, Cl^-, SO_4^{2-}, NO_3^-, and HCO_3^-, relatively low in pH values. Three samples were grouped in this major category which has Mg^{2+}-Na^+-HCO_3^- water types (Table 2). The second Group (G2) is categorized with intermediate values of most parameters which have very low values of K^+ and Ca^{2+}. A total of ten samples are grouped under this major group and is sub groped into G2SB1and G2SB2. G2SB1 include seven samples which are characterized by their high values of Cl^- and NO_3^-, intermediate values for most other parameters. It has Ca^{2+}-Mg^{2+}-HCO_3^- water types. This subgroup could of groundwater contamination from agriculture activities. G2SB2 include three samples categorized under which is characterized by low values of Na^+, K^+, SO_4^{2-}, and high values Ca^{2+}, HCO_3^-, and EC with intermediate values of the other parameters. It has a Ca^{2+}-Mg^{2+}-HCO_3^- water type. It is sourced from the lower water bearing basalt formation with Ca^{2+}-Mg^{2+} rich silicate minerals (Table 2).

Table 2 List of the major groups and their subgroups with a number of samples and descriptions

SN.	Major Groups	Sub Groups	Samples ID	No of Samples	Description,
1	G1		KW8, KW9, and HG10	3	Mg^{2+}-Na^{+}-HCO_3^{-} water type, Elevated EC, Na^{+}, Mg^{2+}, Cl^{-}, SO_4^{2-}, NO_3^{-}, and HCO_3^{-}
2	G2	G2SB1	KW5, HG25, HG24, HG33, HG22, HG21, and HG18	7	Ca^{2+}-Mg^{2+}-HCO_3^{-} water type, low values of K^{+}, elevated Cl^{-}, and NO_2^{-}
3		G2SB2	KW3, HG17, and HG16	3	Ca^{2+}-Mg^{2+}-HCO_3^{-} water type, low values of Na^{+}, K^{+}, SO_4^{2-}, and elevated Ca^{2+}, HCO_3^{-}, and EC.
4	G3		KW2, KW1, HG26, and HG12	4	Ca^{2+}-Mg^{2+}-HCO_3^{-} water type, low NO_3^{-}, and high K^{+}
5	G4	G4SB1	GS, BH1, BH2 and KW6	4	Na^{+}-HCO_3^{-} water types, Spring and artesian wells, elevated Na^{+} and pH, low values of HCO_3^{-}, Ca^{2+}, Mg^{2+}, K^{+}, NO_3^{-}, TDS, and EC
6		G4SB2	HG15, KW10, KW4, HG13, HG19, HG11, HG29, HG8, HG20, KW7, HG33, HG14, and HG28	13	Mg^{2+}-Ca^{2+}-HCO_3^{-} water type, low EC, TDS, Na^{+}, K^{+}, Cl^{-}, and SO_4^{2-}
Total number of samples				34	

The third Group (G3) includes four samples which and are grouped based on their similarity in having a low concentration of NO_3^{-} and K^{+}, intermediate values of the remaining parameters. It is also a Ca^{2+}-Mg^{2+}-HCO_3^{-} water type. It is possible to understand that the sources of the groundwater chemistry are from calcium-magnesium rich pyroxene phyric basalt weathering and the boreholes are located near the western mountainous of the basalt formation (Table 2). The fourth group (G4) groundwater samples are divided into two subgroups namely G4SB1 and G4SB2. G4SB1 contains four samples with a high concentration of Na^{+} and HCO_3^{-}, but low EC, TDS, Ca^{2+}, and Mg^{2+}. It has Na^{+}-HCO_3^{-} water types which reveal that the groundwater is from the sodium rich silicate weathering (acidic rocks), due to the long groundwater flow path from the recharge to the discharge. The samples from the artesian wells and springs in the

study area were grouped in G4SB1 subgroup. G4SB2 contains thirteen samples and has Mg^{2+}-Ca^{2+}-HCO_3^- water types which is the dominant water type and subgroup in the Golina River Basin. This groundwater is obtained from the olivine-rich water-bearing basalts formation (Table 2).

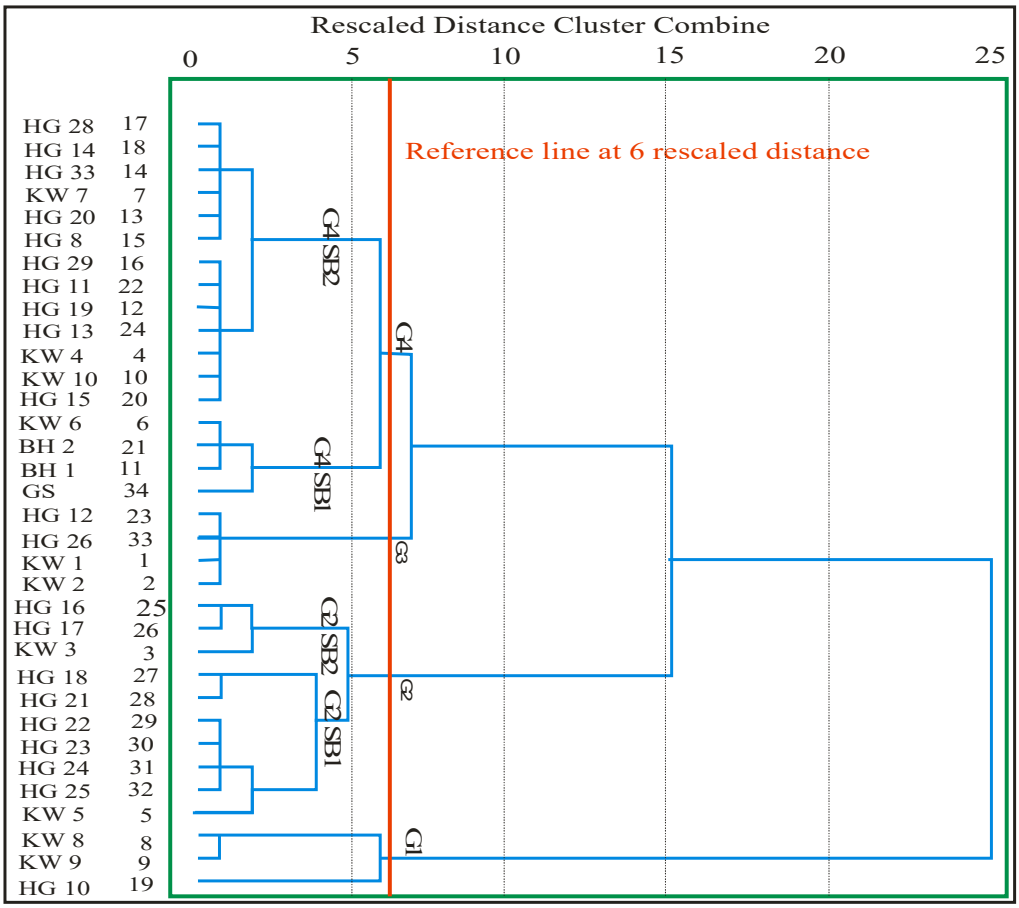


Figure 9. Dendrogram used for the clustering of water samples using Ward's linkage and squared Euclidian distance measurement.

3.2. $\delta^{18}O$ and $\delta^{2}H$ characteristics and groundwater recharge

3.2.1. Precipitation

Several recharge processes may be defined for groundwater systems; however, their respective influence is difficult to determine without a good knowledge of the input signal (i.e., precipitation) (Clark & Fritz, 1997). Considering this, the stable water isotopes were determined from the precipitation as well as from groundwater. During the observation period, the $\delta^{18}O$ and $\delta^{2}H$ in precipitation varied from -8.2‰ to +3.6‰ for $\delta^{18}O$ and -51.1‰ to +31.8‰ for $\delta^{2}H$ (Table 3; Figure 11a). The d-excess of the precipitation ranged from -1.66 to +21.42‰ (Figure 11b). Similarly, the precipitation in summer has a value of stable isotopes for $\delta^{2}H$

which varies from -51.12 $^{0}/_{00}$ to +31.8$^{0}/_{00}$ and for $\delta^{18}O$ varies from -8.22 to +3.62$^{0}/_{00}$. The winter precipitations have a value of stable isotopes for $\delta^{2}H$ which varies from -0.03 to +28.72$^{0}/_{00}$ and for $\delta^{18}O$ varies from -1.28 to +2.95$^{0}/_{00}$. It is observed that precipitation events between June and September are relatively more depleted in heavy isotopes than rest of the month's precipitation (Figure 11a). This is due to the seasonal climate variations and changes in moisture sources, resulting significant variance in the d-excess of precipitation events in the GRB.

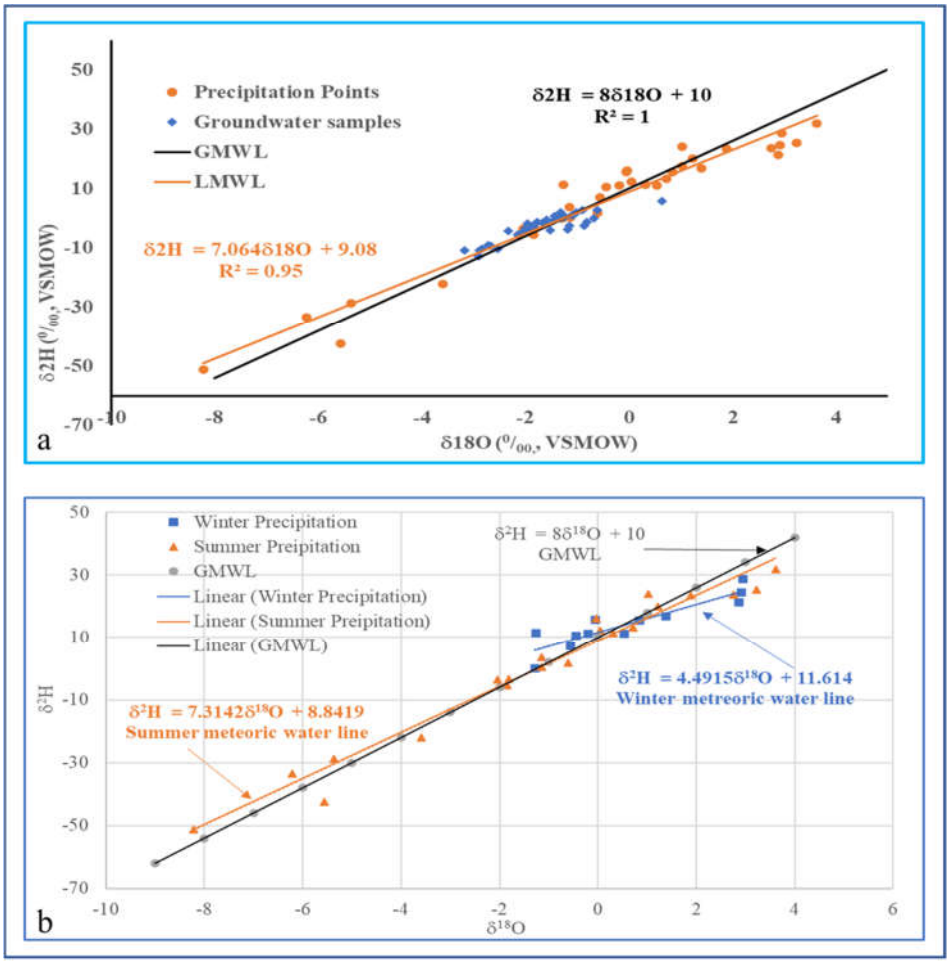


Figure 10. Global meteoric water line (a) Local meteoric water line (LMWL) and (b) with seasonal meteoric water lines of the Golina River Basins

Stable isotopes ($\delta^{18}O$ and $\delta^{2}H$) in precipitation and river water are variables that provide information about hydrological processes, such as flow, evaporation, water supply, and the connectivity between aquifers within a catchment, and surface-groundwater interactions, salinity and mixing (Kebede, 2013; Kendall & Coplen, 2001). The slope (8) and deuterium excess (10) vary in nature due to a superposition of equilibrium and kinetic isotope effects

depending on the conditions of evaporation, vapor transport, and precipitation. The global meteoric water line (GMWL) described by the condensation of water vapor under conditions close to equilibrium and that was evaporated under conditions of non-equilibrium (Dansgaard, 1964). It provides a convenient reference for understanding and tracing the origin of the water. The slope is related to the ratio of the fractionation coefficients and to factors relating to whether the water entering the soil, groundwater, and lakes have experienced evaporation. The evaporation of soil or lake waters has a slope less than 8 (generally between 4 and 7) (Blasch & Bryson, 2007; Lee et al., 2010). The other important term is the y-intercept (d-excess) and defined by the deviation of isotopic equilibrium during evaporation from sourced precipitation and is related to the relative humidity parameter of the vapor source for evaporation (Dansgaard, 1964).

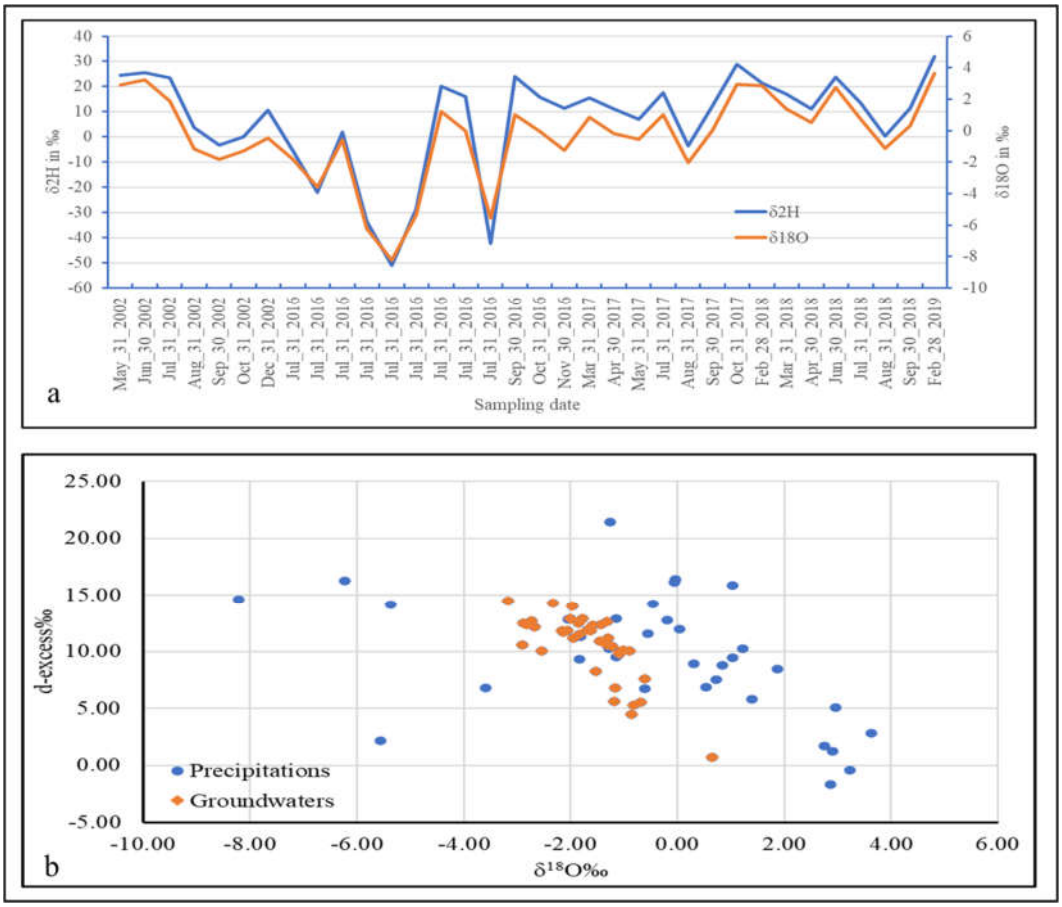


Figure 11. (a) Stable isotopes concentrations of precipitation and (b) relation between delta $\delta^{18}O‰$ and d-excess‰ of precipitation and groundwater from Golina River Basin

The local meteoric water lines of the study area for summer season have a slope of 7.3 with an intercept of 8.8 (Figure 10b) and is expressed as indicated in next equation (Eq. 9). In this case,

both slope and y-intercepts of the regression line of the summer precipitation are similar or close to the global meteoric water line which shows less or no impact of evaporation.

$$\delta^{2}H = 7.3 \pm 4.4\delta^{18}O + 8.8 \pm 1 \quad \text{(Eq. 9)}$$

The slope and intercept of the dry season local meteoric water line of the area are 4.5 and 11.6, respectively (Figure 10b). The local meteoric water line during dry season precipitation of the Golina River Basin shows a significant deviation from the global meteoric water line due to the evaporation effect on the rainwater droplets. It gives an enrichment of heavy isotopes of $\delta^{2}H$ and $\delta^{18}O$ in the precipitation during the dry season because of the high temperature of the atmosphere and relative humidity. The linear regression line of the stable isotopes of precipitation in dry season is expressed as the following equation (Eq. 10).

$$\delta^{2}H = 4.5 \pm 3.5\delta^{18}O + 11.6 \pm 1.1 \quad \text{(Eq. 10)}$$

It clearly shows the evaporation effect on the stable isotopes of the precipitation during the winter season to enrich in heavy isotopes (Figure 10b and 11a). By combining all precipitation water sample data, the local meteoric water line (LMWL) of the GRB is developed (Figure 10a and Figure 12). As a result, the slope and d-excess values of the MWL equation of Golina River Basin are smaller than that of the equation of the MWL of the globe as shown in equation (Eq. 11).

$$\delta^{2}H = 7.06 \pm 4.75\delta^{18}O + 9.08 \pm 0.82 \quad \text{(Eq. 11)}$$

3.2.2. Groundwater

The values of the $\delta^{2}H$ in groundwater in the study area ranged from -12.68 to +5.80 with an average value of -2.81 $^{0}/_{00}$ while $\delta^{18}O$ in groundwater varies from a max +0.64 to a minimum -3.17 with an average value of -1.66$^{0}/_{00}$ (Table 3). The d-excess of the groundwater samples varies from +0.68$^{0}/_{00}$ to +14.48$^{0}/_{00}$ with an average value of 10.46$^{0}/_{00}$. The relationship between groundwater stable isotope of $\delta^{2}H$ and $\delta^{18}O$ are expressed using the following equation (Eq. 12) so-called Groundwater line (GWL) and plotted in Figure 12.

$$\delta^{2}H = 5.1 \pm 2\delta^{18}O + 5.67 \pm 0.77 \quad \text{(Eq. 12)}$$

Most of the groundwater samples from the study area lie above and near the local meteoric water lines which indicates the groundwater is meteoric in origin except for few samples that lie under the local meteoric water lines which indicated evaporation effects which could be

coming from recharge in the western mountainous (Figure 12). It was also noted that most of the groundwater samples have a deuterium excess (d-value) with a range of 10±3 which is close to global y-intercept and indicated that the groundwater is a meteoric origin with a little or no imprint kinetic evaporation. Therefore, the stable isotopes of the groundwater in the study area indicate mainly meteoric water in origin and to some extent evaporated groundwater coming from recharge in the western mountainous areas.

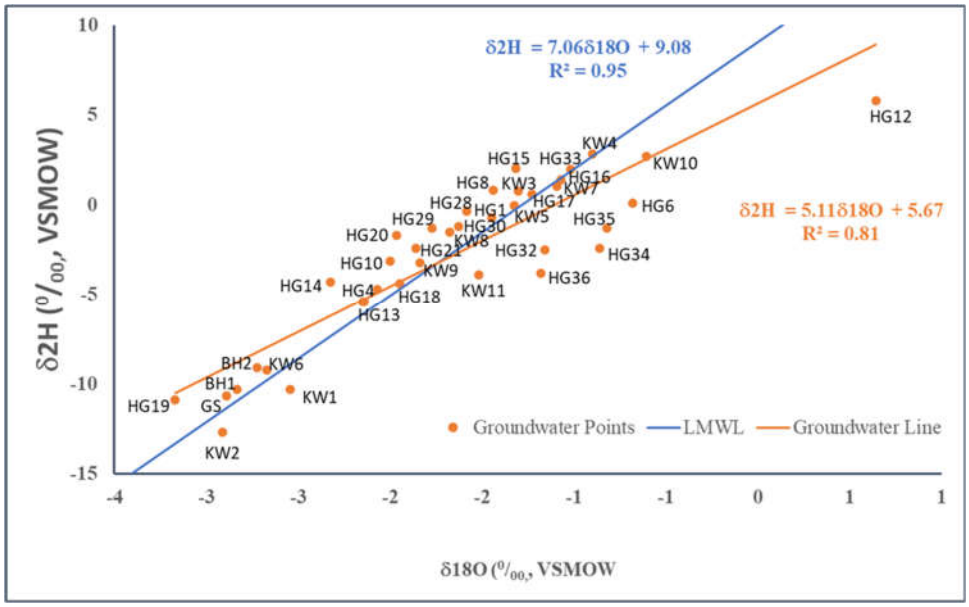


Figure 12 Local meteoric water line (LMWL) and groundwater lines (GWL) of the study area

Table 1 Analytical results of stable isotopes in Precipitation and Groundwater

Precipitation water samples							Groundwater samples						
S.ID	X	Y	Z	δ 2H	δ 18O	d-excess	S.ID	X	Y	Z	δ 2H	δ 18O	d-excess
KP1	576264	1339071	1475	-5.46	-1.84	9.29	BH1	575951	1334484	1372	-10.3	-2.83	12.36
KP2	574052	1330810	1501	-21.99	-3.6	6.78	KW1	576264	1339071	1385	-10.33	-2.54	10.01
KP3	574031	1331626	1426	1.85	-0.61	6.75	KW2	574052	1330810	1449	-12.68	-2.91	10.6
KP4	568499	1328446	1618	-33.48	-6.22	16.29	KW3	574031	1331626	1414	0.77	-1.3	11.2
KP5	573586	1335279	1408	-51.12	-8.22	14.62	KW4	568499	1328446	1585	2.85	-0.9	10.07
KP6	552309	1343650	2186	-28.71	-5.36	14.18	KW5	573586	1335279	1399	-0.03	-1.32	10.57
KP7	576201	1334747	1372	19.99	1.22	10.22	KW6	552309	1343650	2187	-9.24	-2.67	12.13
KP8	568168	1339495	1945	16.09	-0.04	16.39	KW7	576201	1334747	1363	1.05	-1.09	9.8
KP9	572694	1347958	1851	-42.39	-5.57	2.14	KW8	568168	1339495	1468	-1.53	-1.68	11.87
KPS1	568909	1341253	1499	24.07	1.03	15.86	KW9	572694	1347958	1498	-3.24	-1.84	11.48
KPS2	568909	1341253	1499	15.69	-0.05	16.11	KW10	577616	1348458	1512	2.72	-0.61	7.57

Continued .....

KPS3	568909	1341253	1499	11.32	-1.26	21.42	HG28	568163	1341138	1491	-0.36	-1.58	12.3
KPS4	568909	1341253	1499	15.53	0.85	8.77	HG29	569012	1341579	1479	-1.27	-1.77	12.9
KPS5	568909	1341253	1499	11.16	-0.2	12.75	HG8	567144	1340237	1520	0.81	-1.44	12.34
KPS6	568909	1341253	1499	7.11	-0.56	11.6	HG33	566668	1338847	1525	2	-1.02	10.14
KPS7	568909	1341253	1499	17.66	1.03	9.45	HG20	568958	1338275	1461	-1.69	-1.96	14.02
KPS8	568909	1341253	1499	-3.57	-2.05	12.82	HG19	574226	1337244	1396	-10.88	-3.17	14.48
KPS9	568909	1341253	1499	12.3	0.04	11.98	HG14	572306	1335796	1412	-4.31	-2.32	14.28
KPS10	568909	1341253	1499	28.72	2.95	5.1	BH2	575950	1334790	1380	-9.12	-2.72	12.67
KPS11	568909	1341253	1499	21.3	2.87	-1.66	HG10	575262	1332335	1375	-3.14	-2	12.86
KPS12	568909	1341253	1499	16.9	1.39	5.78	HG15	575376	1330634	1403	2.05	-1.32	12.6
KPS13	568909	1341253	1499	11.1	0.53	6.86	GS	570506	1333186	1424	-10.66	-2.89	12.46
KPS14	568909	1341253	1499	23.7	2.75	1.7	KW11	573590	1335300	1399	-3.9	-1.52	8.26
KPS15	568909	1341253	1499	13.3	0.72	7.54	HG6	567755	1339869	1495	0.1	-0.68	5.54
KPS16	568909	1341253	1499	0.4	-1.14	9.52	HG12	571590	1336548	1423	5.8	0.64	0.68
KPS17	568909	1341253	1499	11.4	0.31	8.92	HG1	568077	1338926	1477	-0.7	-1.45	10.9
KPS18	568909	1341253	1499	31.8	3.62	2.84	HG4	569350	1339461	1459	-4.7	-2.07	11.86
KPS19	568909	1341253	1499	24.52	2.91	1.24	HG13	572306	1335796	1412	-5.4	-2.14	11.72
KPS20	568909	1341253	1499	25.41	3.23	-0.43	HG11	570604	1337073	1435	-5.4	-2.15	11.8
KPS21	568909	1341253	1499	23.5	1.88	8.46	HG16	574995	1330597	1419	1.4	-1.07	9.96
KPS22	568909	1341253	1499	3.67	-1.15	12.87	HG17	574671	1331878	1394	0.6	-1.23	10.44
KPS23	568909	1341253	1499	-3.28	-1.82	11.28	HG18	574472	1332357	1388	-4.4	-1.95	11.2
KPS24	568909	1341253	1499	-0.03	-1.28	10.21	HG21	572982	1332682	1419	-2.4	-1.86	12.48
KPS25	568909	1341253	1499	10.61	-0.45	14.21	HG30	567688	1338578	1485	-1.2	-1.63	11.84
							HG32	568356	1337982	1464	-2.5	-1.16	6.78
							HG34	569299	1341890	1483	-2.4	-0.86	4.48
							HG35	569892	1341651	1471	-1.3	-0.82	5.26
							HG36	569814	1341065	1464	-3.8	-1.18	5.64

4. CONCLUSIONS

The present study aimed to identify the mineralization processes that determine the dissolved solutes in the groundwater, and comprehend the groundwater recharge mechanism of the Golina River Basin using major ions and stable water isotope approaches. From the molar ratios of the major ions results, concluded the solute sources of the groundwater of the Golina River Basin is derived dominantly from the weathering of Ca^{2+} and Mg^{2+}-rich silicate minerals; most probably pyroxene and olivine minerals of basalts. However, the weathering of Na^{+} and K^{+} -

rich acidic materials has its own contribution for the solute sources of the groundwater in the area. The Gibbs ratios results shows the solute sources of the groundwater in the region controlled by rock dominance which is the interaction between water and rocks (soils). Similarly, the Chloro-alkaline ratios and Durov's diagrams also clearly showed the groundwater chemistry is influenced by the ion exchanges between the aquifer materials and that of groundwater. The HCA approach gave four major groups and 4 subgroups of water based on their physicochemical characteristics. The stable isotopes in precipitation in study area show significant variance between winter (enriched in δ^2H and $\delta^{18}O$) and summer (depleted in δ^2H and $\delta^{18}O$). Hence, the precipitation of the area was affected by evaporation before reaching the soil and infiltrated takes place. The stable isotope analysis of the groundwater samples confirm that the groundwater is meteoric in origin for those samples falling along and close to the local meteoric water line with 10±3 d-excess, while those samples falling below the LMWL indicate that the groundwater is recharged from the evaporation affected sources. Therefore, it is possible to conclude that the groundwater is recharged from direct infiltration and recharged from the nearby mountainous on west and east. Since most of the water samples for major ions and stable isotope analysis were collected from the valley floor, this result mainly refers to this part of the study area. Therefore, it is recommended that the mountainous area should be studied in a better detail by gathering additional water samples.

Acknowledgment

The authors wish to thanks Samara University and Mekelle University for funding the research work. We would also like to extend our appreciation to the Technical University of Darmstadt (TUD) and Addis Ababa University School of Earth Sciences Water Laboratory for their laboratory analysis support.

REFERENCE

Aggarwal, P. K., Gat, J. R., & Froehlich, K. F. O. (2005). Isotopes in the water cycle: Past, present and future of a developing science. In *Isotopes in the Water Cycle: Past, Present and Future of a Developing Science*. https://doi.org/10.1007/1-4020-3023-1

Alemayehu, T., Leis, A., Eisenhauer, A., & Dietzel, M. (2011). Multi-proxy approach (2H/H, 18O/16O, 13C/12C and 87Sr/86Sr) for the evolution of carbonate-rich groundwater in basalt dominated aquifer of Axum area, northern Ethiopia. *Chemie Der Erde*. https://doi.org/10.1016/j.chemer.2011.02.007

Ayenew, T., GebreEgziabher, M., Kebede, S., & Mamo, S. (2013). Integrated assessment of hydrogeology and water quality for groundwater-based irrigation development in the Raya Valley, northern Ethiopia. *Water International*. https://doi.org/10.1080/02508060.2013.821640

Ayenew, T., Kebede, S., & Alemyahu, T. (2008). Environmental isotopes and hydrochemical study applied to surface water and groundwater interaction in the Awash River basin. *Hydrological Processes*. https://doi.org/10.1002/hyp.6716, *22*(8), 1548–1563.

Bawoke, G. T., Anteneh, Z. L., Kehali, A. T., Mohammedyasin, M. S., & Wudie, G. (2019). Hydrogeochemical and isotopic signatures of groundwater in the Andasa watershed, Upper Blue Nile basin, Northwestern Ethiopia. *Journal of African Earth Sciences*. https://doi.org/10.1016/j.jafrearsci.2019.103617

Bedaso, Z. K., DeLuca, N. M., Levin, N. E., Zaitchik, B. F., Waugh, D. W., Wu, S. Y., Harman, C. J., & Shanko, D. (2019). Spatial and temporal variation in the isotopic composition of Ethiopian precipitation. *Journal of Hydrology*, 124364. https://doi.org/10.1016/j.jhydrol.2019.124364

Belkhiri, L., & Mouni, L. (2012). Hydrochemical analysis and evaluation of groundwater quality in El Eulma area, Algeria. *Applied Water Science*, *2*(2), 127–133. https://doi.org/10.1007/s13201-012-0033-6

Birks, S. J., Gibson, J. J., Gourcy, L., Aggarwal, P. K., & Edwards, T. W. D. (2002). Maps and animations offer new opportunities for studying the global water cycle. *Eos, Transactions American Geophysical Union*, *83*(37), 406.

Blasch, K. W., & Bryson, J. R. (2007). Distinguishing sources of ground water recharge by using δ2H and δ18O. *Ground Water*. https://doi.org/10.1111/j.1745-6584.2006.00289.x

Candela, L., & Morell, I. (2009). Basic chemical principles of groundwater. *Encyclopedia of Life Support Systems*, *2*, 43–55.

Clark, I. D., & Fritz, P. (1997). *Environmental isotopes in hydrogeology*. CRC press.

Clark, I. D., & Fritz, P. (2013). Environmental Isotopes in Hydrogeology. In *Environmental Isotopes in Hydrogeology*. https://doi.org/10.1201/9781482242911

Craig, H. (1961). Isotopic variations in meteoric waters. *Science*. https://doi.org/10.1126/science.133.3465.1702

Dansgaard, W. (1964). Stable isotopes in precipitation. *Tellus*. https://doi.org/10.3402/tellusa.v16i4.8993

Demlie, M., Wohnlich, S., & Ayenew, T. (2008). Major ion hydrochemistry and environmental isotope signatures as a tool in assessing groundwater occurrence and its dynamics in a fractured volcanic aquifer system located within a heavily urbanized catchment, central Ethiopia. *Journal of Hydrology*. https://doi.org/10.1016/j.jhydrol.2008.02.009

Fynn, O. F., Yidana, S. M., Chegbeleh, L. P., & Yiran, G. B. (2016). Evaluating groundwater recharge processes using stable isotope signatures—the Nabogo catchment of the White Volta, Ghana. *Arabian Journal of Geosciences*, *9*, 1–15.

Gat, J. R. (1996). OXYGEN AND HYDROGEN ISOTOPES IN THE HYDROLOGIC CYCLE. *Annual Review of Earth and Planetary Sciences*. https://doi.org/10.1146/annurev.earth.24.1.225

Gebru, H., Gebreyohannes, T., & Hagos, E. (2020). Identification of Groundwater Potential Zones Using Analytical Hierarchy Process (AHP) and GIS-Remote Sensing Integration, the Case of Golina River Basin, Northern Ethiopia. *International Journal of Advanced Remote Sensing and GIS*, *9*(1), 3289–3311. https://doi.org/https://doi.org/10.23953/cloud.ijarsg.460

Gibbs, R. J. (1970). Mechanisms controlling world water chemistry. *Science*. https://doi.org/10.1126/science.170.3962.1088

Girmay, E., Ayenew, T., Kebede, S., Alene, M., Wohnlich, S., & Wisotzky, F. (2015). Conceptual groundwater flow model of the Mekelle Paleozoic–Mesozoic sedimentary outlier and surroundings (northern Ethiopia) using environmental isotopes and dissolved ions. *Hydrogeology Journal*. https://doi.org/10.1007/s10040-015-1243-4

Gonfiantini, R. (1998). On the isotopic composition of precipitation. In *Hydrology and isotope geochemistry*.

Gregnanin, A. and, & Piccirillo, E. (1974). *Considerazioni Sulle Serie Vulcaniche E Sulla Struttura Dell'altopiano Etiopico Centrale*.

Helena, B., Pardo, R., Vega, M., Barrado, E., Fernandez, J. M., & Fernandez, L. (2000). Temporal evolution of groundwater composition in an alluvial aquifer (Pisuerga River, Spain) by principal component analysis. *Water Research*. https://doi.org/10.1016/S0043-1354(99)00225-0

Hoffmann, G., Jouzel, J., & Masson, V. (2000). Stable water isotopes in atmospheric general circulation models. *Hydrological Processes*, *14*(8), 1385–1406.

Hofmann, C., Courtillot, V., Féraud, G., Rochette, P., Yirgu, G., Ketefo, E., & Pik, R. (1997). Timing of the ethiopian flood basalt event and implications for plume birth and global change. *Nature*. https://doi.org/10.1038/39853

IAEA. (1983). Guidebook on nuclear techniques in hydrology 1983 edition. *Journal of Hydrology*. https://doi.org/10.1016/0022-1694(86)90086-7

IAEA. (1989). Isotope techniques in the study of the hydrology of fractured and fissured rocks. Proceedings of an advisory group meeting, Vienna, 1986. *Isotope Techniques in the Study of the Hydrology of Fractured and Fissured Rocks. Proceedings of an Advisory Group Meeting, Vienna, 1986*.

Jeelani, G., Deshpande, R. D., Galkowski, M., & Rozanski, K. (2018). Isotopic composition of daily precipitation along the southern foothills of the Himalayas: impact of marine and continental sources of atmospheric moisture. *Atmospheric Chemistry and Physics*, *18*(12), 8789–8805.

Jeelani, G., Shah, R. A., Deshpande, R. D., Fryar, A. E., Perrin, J., & Mukherjee, A. (2017). Distinguishing and estimating recharge to karst springs in snow and glacier dominated mountainous basins of the western Himalaya, India. *Journal of Hydrology*, *550*, 239–252.

Kebede, S. (2013). Groundwater in Ethiopia: Features, numbers and opportunities. https://doi.org/10.1007/978-3-642-30391-3

Kebede, S., Travi, Y., Alemayehu, T., & Ayenew, T. (2005). Groundwater recharge, circulation and geochemical evolution in the source region of the Blue Nile River, Ethiopia. *Applied Geochemistry*. https://doi.org/10.1016/j.apgeochem.2005.04.016

Kebede, S., Travi, Y., Asrat, A., Alemayehu, T., Ayenew, T., & Tessema, Z. (2008). Groundwater origin and flow along selected transects in Ethiopian rift volcanic aquifers. *Hydrogeology Journal*. https://doi.org/10.1007/s10040-007-0210-0

Kehew, A. E. (2001). Applied Chemical Hydrogeology. *Prentice-Hall*. https://doi.org/10.1006/nbdi.2000.0328

Kendall, C., & Coplen, T. B. (2001). Distribution of oxygen-18 and deuteriun in river waters across the United States. *Hydrological Processes*. https://doi.org/10.1002/hyp.217

Krishna kumar, S., Logeshkumaran, A., Magesh, N. S., Godson, P. S., & Chandrasekar, N. (2015). Hydro-geochemistry and application of water quality index (WQI) for groundwater quality assessment, Anna Nagar, part of Chennai City, Tamil Nadu, India. *Applied Water Science*. https://doi.org/10.1007/s13201-014-0196-4

Kuang, X., Luo, X., Jiao, J. J., Liang, S., Zhang, X., Li, H., & Liu, J. (2019). Using stable isotopes of surface water and groundwater to quantify moisture sources across the Yellow River source region. *Hydrological Processes*. https://doi.org/10.1002/hyp.13441

Kumar, M., Kumari, K., Singh, U. K., & Ramanathan, A. (2009). Hydrogeochemical processes in the groundwater environment of Muktsar, Punjab: Conventional graphical and multivariate statistical approach. *Environmental Geology*. https://doi.org/10.1007/s00254-008-1367-0

Lee, J., Feng, X., Faiia, A. M., Posmentier, E. S., Kirchner, J. W., Osterhuber, R., & Taylor, S. (2010). Isotopic evolution of a seasonal snowcover and its melt by isotopic exchange between liquid water and ice. *Chemical Geology*. https://doi.org/10.1016/j.chemgeo.2009.11.011

Liu, Z., Bowen, G. J., & Welker, J. M. (2010). Atmospheric circulation is reflected in precipitation isotope gradients over the conterminous United States. *Journal of Geophysical Research: Atmospheres*, *115*(D22).

Matthess, G. (1982). *The property of Groundwater* (No. 551.49).

McGuire, K. J., DeWalle, D. R., & Gburek, W. J. (2002). Evaluation of mean residence time in subsurface waters using oxygen-18 fluctuations during drought conditions in the mid-Appalachians. *Journal of Hydrology*, *261*(1–4), 132–149.

Meybeck, M. (1987). Global chemical weathering of surficial rocks estimated from river dissolved loads. *American Journal of Science*. https://doi.org/10.2475/ajs.287.5.401

Price, R. M., & Swart, P. K. (2006). *Geochemical indicators of groundwater recharge in the surficial aquifer system, Everglades National Park, Florida, USA*.

Redwan, M., & Abdel Moneim, A. A. (2016). Factors controlling groundwater hydrogeochemistry in the area west of Tahta, Sohag, Upper Egypt. *Journal of African Earth Sciences*, *118*, 328–338. https://doi.org/10.1016/j.jafrearsci.2015.10.002

Schoeller, H. (1967). Qualitative Evaluation of Groundwater. In: Resources.Methods and Techniques of Groundwater Investigation and Development. *Water Resources*, *33*, 44–52.

Shah, R. A., Jeelani, G., & Jacob, N. (2017). Estimating mean residence time of karst groundwater in mountainous catchments of Western Himalaya, India. *Hydrological Sciences Journal*, *62*(8),

1230–1242.
Shah, R. A., Jeelani, G., Yadav, J. S., & Rai, S. K. (2022). Hydrogeochemical and stable isotopic evidence to different water origins of karst springs in the western Himalayas, India. *Environmental Earth Sciences*, *81*(10), 297.
Shah, R. A., Rai, S. K., & Yadav, J. S. (2023). Understanding recharge processes and solute sources of groundwater in karst settings of the Lesser Himalaya, India. *Arabian Journal of Geosciences*, *16*(3), 186.
Singhal, B. B. S., & Gupta, R. P. (2010). Applied hydrogeology of fractured rocks: Second edition. In *Applied Hydrogeology of Fractured Rocks: Second Edition*. https://doi.org/10.1007/978-90-481-8799-7
Tóth, J. (1999). Groundwater as a geologic agent: An overview of the causes, processes, and manifestations. In *Hydrogeology Journal*. https://doi.org/10.1007/s100400050176.
Zanettin, B. A., & Justin-Visentin, E. (1973). Serie di vulcaniti etiopiche; 1, La serie dell'altipiano etiopico centro-orientale. *Bollettino Della Società Geologica Italiana*, *92.2*, 313–327.

Publisher's Note

Daagu International Journal of Basic and Applied Research remains neutral with regard to jurisdictional claims in published maps and institutional affiliations.